Hydrogen bonding in selected vanadates- a Raman and infrared spectroscopy study

Ray L. Frost• , Kristy Erickson, Matt L. Weier

Inorganic Materials Research Program, School of Physical and Chemical Sciences, Queensland University of Technology, GPO Box 2434, Brisbane Queensland 4001, Australia.

Published as:
Frost R. L., Erickson K.L. & Weier, M. Hydrogen bonding in selected vanadates: a Raman and infrared spectroscopy study. Spectrochimica acta. Part A, Molecular and biomolecular spectroscopy, 2004. 60(10): p. 2419-23.

Abstract

Water plays an important role in the stability of minerals containing the deca and hexavanadates ions. A selection of minerals including pascoite, huemulite, barnesite, hewettite, metahewettite, hummerite has been analysed. Infrared spectroscopy combined with Raman spectroscopy has enabled the spectra of the water HOH stretching bands to be determined. The use of the Libowitzky type function allows for the estimation of hydrogen bond distances to be determined. The strength of the hydrogen bonds can be assessed by these hydrogen bond distances. An arbitrary value of 2.74 Å was used to separate the hydrogen bonds into two categories such that bond distances less than this value are considered as strong hydrogen bonds whereas hydrogen bond distances greater than this value are considered relatively weaker. Importantly infrared spectroscopy enables the estimation of hydrogen bond distances using an empirical function.

Keywords: pascoite, huemulite, barnesite, hewettite, metahewettite, hummerite, vanadates, Raman spectroscopy, infrared spectroscopy

---

1. Introduction

Vanadium in minerals represents the most complicated of systems because of the variable oxidation state of vanadium, and many of the minerals have been identified around a century ago [1-3]. This complication is exacerbated by the range of oxidation states in the natural environment, including the supergene zone. These include V(III), V(IV), V(V). Polymerisation of V(V) as $(VO_4)^{3-}$, in more concentrated solutions, gives rise to three types of complex anions. If the pH is between 9 and 13, pyrovanadates [$(V_2O_7)^{4-}$, $(HV_2O_7)^{3-}$,$(H_2V_2O_7)^{2-}$] are formed, in the pH range 5 to 9 metavanadates [$(V_3O_9)^{3-}$, $(V_4O_{12})^{4-}$, $(H_2V_3O_{10})^{3-}$, $(HV_3O_{10})^{4-}$,$(V_5O_{15})^{5-}$,] are predominantly formed, and as solutions become more acidic decavanadates [$(V_{10}O_{28})^{6-}$] are formed. Huemulite ($Na_4MgV_{10}O_{28}.24H_2O$) is a simple salt of the

• Author for correspondence (r.frost@qut.edu.au)

decavanadate isopolyanion $(V_{10}O_{28})^{6-}$ [4] . Other vanadium minerals may precipitate out from solution. These include the so-called hexavandates which are based upon polymeric $(V_6O_{16})^{2-}$ and contain distorted layers of VO_5 and VO_6 polyhedra [5]. A somewhat similar polymeric structure occurs in the formation of $(V_5O_{14})^{3-}$ ions with the vanadium coordination spheres being tetrahedral and square planar. Minerals which correspond to these types of salts are barnesite ($Na_2V_6O_{16}.3H_2O$) , hewettite ($CaV_6O_{16}.9H_2O$) [6-9], metahewettite ($CaV_6O_{16}.H_2O$), hummerite ($KMgV_5O_{14}.8H_2O$) [10].

Each of the minerals listed above contains water molecules in the formula unit. Hydrogen plays an extremely important role in the structure and chemistry of oxysalt minerals such as for these vanadates. The presence of water adds to the stability of the oxysalt [11]. For any crystal structure the structural unit may be defined as the strongly bonded part of the unit. Structural units are linked together by interstitial species such as univalent and divalent cations and by water groups that are involved in much weaker bonding. Studies have shown a strong correlation between OH stretching frequencies and both the O···O bond distances and the H···O hydrogen bond distances. [12-15] The elegant work of Libowitzky (1999) showed that a regression function can be employed relating the above correlations with regression coefficients better than 0.96 [16]. The function is $\nu_1 = 3592\text{-}304x109\exp(\text{-}d(O\text{-}O)/0.1321)$ cm^{-1}. Two types of OH units are identified in the structure and the known hydrogen bond distances used to predict the hydroxyl stretching frequencies.
The structures and chemistry of the minerals containing vanadates is both impressive in both their complexity and diversity. As Hawthorne rightly points out our knowledge and understanding of the role of water in minerals lags far behind experimental capabilities [11]. It is interesting that Farmer in his tome on the infrared spectroscopy of minerals did not list the band positions of water in the decavanadates [17]. As part of our on-going studies of the vibrational spectroscopy of minerals particularly secondary minerals, we report the Raman and infrared spectra of the hydroxyl stretching and bending region of selected vanadium containing minerals including pascoite, huemulite, barnesite, hewettite, metahewettite and hummerite. The Raman spectra are then related to the mineral structure.

2. Experimental

2.1 Minerals

The minerals are listed in the table below and were analysed for phase purity by X-ray diffraction and for composition by using the electron probe.

Mineral	Formula	Place of origin
Barnesite	$Na_2V_6O_{16}.3H_2O$	Cactus Rat Mine, Thompson district, Grand County, Utah, USA
Hewettite	$CaV_6O_{16}.9H_2O$	Parco #8 Mine, Yellow cat District. Thompson, Grand County, Utah, USA
Metahewettite	$CaV_6O_{16}.H_2O$	Parco #8 Mine, Yellow cat District. Thompson, Grand County, Utah, USA

Huemulite	$Na_4MgV_{10}O_{28}.24H_2O$	The Fish, Eureka County, Nevada, USA
Hummerite	$KMgV_5O_{14}.8H_2O$	Hummer Mine, Paradox valley. Montrose County, Colarado, USA
Pascoite	$Ca_3V_{10}O_{28}.17H_2O$	La Sal District, San Juan County, Utah, USA
Rossite	$CaV_2O_6.4H_2O$	Burro Mine, Slick Rock, San Miguel County, Colarado, USA
Metarossite	$CaV_2O_6.2H_2O$	Burro Mine, Slick Rock, San Miguel County, Colarado, USA

2.2 Infrared absorption spectroscopy

Infrared absorption spectra were obtained using the KBr pressed pellet technique using a Perkin-Elmer FT-IR spectrometer 2000 bench using 4 cm^{-1} resolution with 128 scans. Diffuse Reflectance Fourier Transform Infrared spectroscopic (commonly known as DRIFT) analyses were undertaken using a Bio-Rad 60A spectrometer. 512 scans were obtained at a resolution of 2 cm^{-1} with a mirror velocity of 0.3 cm/sec. Spectra were co-added to improve the signal to noise ratio.

2.3 Raman microprobe spectroscopy

The crystals of the vanadate minerals were placed and orientated on the stage of an Olympus BHSM microscope, equipped with 10x and 50x objectives and part of a Renishaw 1000 Raman microscope system, which also includes a monochromator, a filter system and a Charge Coupled Device (CCD). Raman spectra were excited by a HeNe laser (633 nm) at a resolution of 2 cm^{-1} in the range between 100 and 4000 cm^{-1}. Repeated acquisition using the highest magnification was accumulated to improve the signal to noise ratio. Spectra were calibrated using the 520.5 cm^{-1} line of a silicon wafer. In order to ensure that the correct spectra are obtained, the incident excitation radiation was scrambled. Previous studies by the authors provide more details of the experimental technique. Spectra at controlled temperatures were obtained using a Linkam thermal stage (Scientific Instruments Ltd, Waterfield, Surrey, England). Details of the technique have been published by the authors [18-23]. Spectral manipulation such as baseline adjustment, smoothing and normalisation was performed using the GRAMS® software package (Galactic Industries Corporation, Salem, NH, USA).

3. Results and discussion

Whilst the infrared spectra of the wavenumber region of vanadates up to 1200 cm^{-1} has been published [24], no results of the water OH stretching or bending region has been forthcoming. The infrared spectra of selected naturally occurring decavanadates are shown in Figure 1. The results of the band component analyses of the spectra of the HOH stretching region are reported in Table 1. The regression function of Libowitzky was also used to calculate predicted hydrogen bond distances. These bond distances (Å) are also shown in Table 1.

Four HOH stretching bands are observed for pascoite at 3571, 3435, 3261 and 3067 cm^{-1} with relative intensities of 3.2, 21.6, 1.1 and 74.0 %. Four Raman bands are observed at 3566, 3465, 3252, 3127 and 3039 cm^{-1} (Figure 2). These bands have relative intensities of 9.8, 35.3, 20.9, 1.5, 12.5, and 20.0 % respectively. The first three bands and the last band in the infrared match reasonably well with the band positions in the Raman spectrum. Thus if we calculate the hydrogen bond distances using the Libowitzky type formula, the 3571 cm^{-1} band provide a hydrogen bond distance of 3.09 Å, 3435 cm^{-1} gives 2.824 Å, 3261 cm^{-1} gives 2.726 Å, and 3067 cm^{-1} 2.665 Å. The infrared spectra show overlap of broad bands in the HOH stretching region. In comparison, the Raman spectra show better band separation with the bandwidths being much less than the bandwidths in the infrared spectrum. The Raman spectrum of pascoite may be divided into two groups of OH stretching wavenumbers: namely 3300 to 3700 cm^{-1} and 2900 to 3300 cm^{-1}. This distinction suggests that the strength of the hydrogen bonds as measured by the hydrogen bond distances can also be divided into two groups according to the H-bond distances. An arbitrary cut-off point may be 2.74 Å based upon the wavenumber 3300 cm^{-1}. Thus the hydrogen bond distances 3.09 and 2.824 Å may be described as weak hydrogen bonding and the bond distances of 2.726 and 2.665 Å as stronger hydrogen bonds.

For the mineral hummerite, four infrared bands are observed at 3541, 3416, 3217 and 2974 cm^{-1}. The relative intensities of these bands are 7.98, 12.94, 40.84 and 38.22 %. The Raman spectrum shows more complexity with bands observed at 3599, 3526, 3416, 3404, 3230, 3223, 3196, 2929 and 2902 cm^{-1}. Four of the infrared bands match with the positions of four of the Raman bands. Hence by using the wavenumbers of the four infrared bands, hydrogen bond distances of 2.973, 2.809, 2.709 and 2.643 Å are obtained. It is suggested that two of the hydrogen bonds are strong (2.709 and 2.643 Å) compared with two hydrogen bonds (2.973 and 2.809 Å). The relative intensities of the infrared bands show that the amount of strong hydrogen bonding is significantly greater than the amount of weak hydrogen bonding.
The infrared spectrum of barnesite shows four bands at 3516, 3396, 3330, 3248 and 3109 cm^{-1} with relative intensities of 30.6, 28.0, 11.5, 16.7 and 13.0 % respectively. Raman bands are observed at 3494, 3435, 3403, 3330 and 3253 cm^{-1}. The relative intensities of these bands are 1.0, 37.2, 53.6, 4.1 and 4.0 %. In the case of barnesite, the position of the infrared bands does not match the positions of the Raman bands. The predicted hydrogen bond distances for barnesite are 2.920, 2.795, 2.757, 2.721 and 2.673 Å. Four of these values are above 2.74 Å. This suggests that the hydrogen bonding in barnesite is significantly weaker than for either pascoite or hummerite.
For metarossite four infrared bands are found at 3526, 3387, 3181, and 2867 cm^{-1}. The relative intensities of these bands are 2.3, 6.9, 60.1 and 30.6%. Three Raman bands are observed at 3473, 3401 and 3177 cm^{-1} with relative intensities of 22.2, 69.6 and 8.15% respectively. The hydrogen bond distances determined from the position of the infrared bands are 2.9393, 2.7995, 2.6977 and 2.6227 Å. As with pascoite and hummerite two types of hydrogen bonding are suggested based upon the hydrogen bond distances, namely two strong hydrogen bonds with distances shorter than 2.74 Å and two comparatively weaker hydrogen bonds with H-bond distances somewhat longer. A similar situation exists for metahewettite with four infrared bands observed at 3537, 3420, 3229 and 2933 cm^{-1}. These bands give hydrogen bond distances of 2.963, 2.812, 2.714 and 2.635 Å.

The presence of water in vanadates is important and it's bonding with the vanadate surface is of necessity for the stability of the mineral layered structure. The region from around 1600 to 1750 cm^{-1} is a window, which is clear of other possible vibrations and is unique in that this is the region where the hydroxyl deformation modes of water are found. As may be observed above, minerals containing physically adsorbed water give strong infrared bands at 3450 cm^{-1}, the water hydroxyl stretching vibration, and at ~ 1630 cm^{-1}, the water bending vibrations. These wavenumber positions are influenced by the amount of adsorbed water, the mineral type and the exchangeable cation to which the water is bonded. For monomeric non-hydrogen bonded water as occurs in the vapour phase, these bands are found at 3755 and 1595 cm^{-1}. For liquid water the bands occur at 3455 and 1645 cm^{-1} and for water molecules in ice, the bands are at 3255 and 1655 cm^{-1}. When water molecules are very tightly bound to the mineral surface as may occur with autunites, then bands occur in the 3200 to 3250 cm^{-1} region. What is being distinguished here is the formation of strong and weak hydrogen bonds. The hydroxyl stretching modes of weak hydrogen bonds occur in the 3580 to 3500 cm^{-1} region and the hydroxyl stretching modes of strong hydrogen bonds occurs below 3420 cm^{-1}. When the water is coordinated to the cation in the clays as occurs in certain minerals, then the water OH stretching frequency occurs at 3220 cm^{-1}. A simple observation can be made that as the water OH stretching frequency decreases then the HOH bending frequency increases. The 3220 cm^{-1} band corresponds to an ice-like structure with O-H···O bond distances of 2.77 Å. Thus the water hydroxyl stretching and the water HOH bending 1610 cm^{-1} frequencies provide a measure of the strength of the bonding of the water molecules either chemically or physically to the vanadate surfaces or to the interlayer anions. Likewise the position of the water bending vibration also provides a measure of this strength of water hydrogen bonding. Bands that occur at frequencies above 1650 cm^{-1} are indicative of coordinated water and chemically bonded water. Bands that occur below 1630 cm^{-1} are indicative of water molecules that are not as tightly bound. In this case the hydrogen bonding is less as the frequency decreases.

Accordingly the infrared spectra of the hydroxyl deformation region are shown in Figure 3. The infrared spectrum of pascoite shows a single band for the HOH deformation modes at 1635 cm^{-1}. The band position is higher than the position for liquid water by around 7 cm^{-1}, indicating the water is more strongly hydrogen bonded compared with the bonding in water. The infrared spectrum of hummerite shows a hydroxyl deformation mode at 1621 $cm^{-1}$with a broad band at 1600 cm^{-1}. The position of these bands would indicate weak hydrogen bonding. In contrast two distinct bands are observed at 1682 and 1619 cm^{-1} for the hydroxyl deformation modes of water in barnesite. The position of the band at 1682 cm^{-1} indicates strong hydrogen bonding. The mineral metarossite also shows a high wavenumber band at 1651 cm^{-1}. The position of the bands for metahewettite is in similar positions to that for hummerite.

4. Conclusions

A series of structurally related minerals including pascoite, huemulite, barnesite, hewettite, metahewettite, hummerite have been studied in the water HOH stretching region by both infrared and Raman spectroscopy. The spectra of the OH stretching region of these minerals show complexity with a number of overlapping bands which are deconvoluted into component bands. The position of these bands

was then used to calculate hydrogen bond distances between the water OH units and the deca or hexavanadates ions. Such hydrogen bond distances are not known and no comparison with distances based upon single crystal X-ray data or neutron scattering data can be made [10]. Importantly infrared spectroscopy enables the estimation of hydrogen bond distances using an empirical function.

Acknowledgements

The financial and infra-structure support of the Queensland University of Technology Inorganic Materials Research Program of the School of Physical and Chemical Sciences is gratefully acknowledged. The Australian Research Council (ARC) is thanked for funding. Museum Victoria is thanked for the loan of the minerals.

References

[1]. W. F. Hillebrand, H. E. Merwin and F. E. Wright, Zeitschrift fuer Kristallographie und Mineralogie 54 (1914) 209.
[2]. W. F. Foshag and F. L. Hess, Proc. U. S. Nat. Museum 72 (1927) 1.
[3]. W. H. Barnes, Am. Mineralogist 40 (1955) 689.
[4]. C. E. Gordillo, E. Linares, R. O. Toubes and H. Winchell, American Mineralogist 51 (1966) 1.
[5]. H. T. Evans, Jr. and M. E. Mrose, Acta Cryst. 11 (1958) 56.
[6]. M. M. Qurashi, Canadian Mineralogist 6 (1961) 647.
[7]. A. Weiss, K. Hartl and E. Michel, Zeitschrift fuer Naturforschung 16b (1961) 842.
[8]. H. G. Bachmann and W. H. Barnes, Canadian Mineralogist 7 (1962) 219.
[9]. P. Bayliss, Mineralogical Magazine 46 (1982) 503.
[10]. J. M. Hughes, M. Schindler, J. Rakovan and F. E. Cureton, Canadian Mineralogist 40 (2002) 1429.
[11]. F. C. Hawthorne, Zeitschrift fuer Kristallographie 201 (1992) 183.
[12]. J. Emsley, Chemical Society Reviews 9 (1980) 91.
[13]. H. Lutz, Structure and Bonding (Berlin, Germany) 82 (1995) 85.
[14]. W. Mikenda, Journal of Molecular Structure 147 (1986) 1.
[15]. A. Novak, Structure and Bonding (Berlin) 18 (1974) 177.
[16]. E. Libowitsky, Monatschefte fÜr chemie 130 (1999) 1047.
[17]. V. C. Farmer, *Mineralogical Society Monograph 4: The Infrared Spectra of Minerals*, 1974.
[18]. R. L. Frost, M. Crane, P. A. Williams and J. T. Kloprogge, Journal of Raman Spectroscopy 34 (2003) 214.
[19]. R. L. Frost, P. A. Williams and W. Martens, Mineralogical Magazine 67 (2003) 103.
[20]. W. Martens, R. L. Frost and J. T. Kloprogge, Journal of Raman Spectroscopy 34 (2003) 90.
[21]. W. Martens, R. L. Frost, J. T. Kloprogge and P. A. Williams, Journal of Raman Spectroscopy 34 (2003) 145.
[22]. R. L. Frost, W. Martens, J. T. Kloprogge and P. A. Williams, Journal of Raman Spectroscopy 33 (2002) 801.

[23]. R. L. Frost, W. Martens, P. A. Williams and J. T. Kloprogge, Mineralogical Magazine 66 (2002) 1063.
[24]. L. D. Frederickson, Jr. and D. M. Hausen, Anal. Chem. 35 (1963) 818.

pascoite			**hummerite**			**barnesite**			**meta rossite**			**meta hewettite**		
IR	H bond Distance/ Å	Raman	IR	H bond Distance/ Å	Raman	IR	H bond Distance/ Å	Raman	IR	H bond Distance/ Å	Raman	IR	H bond Distance/ Å	Raman
3571	3.090_0	3566			3599	3516	2.920_6	3494	3526	2.9393		3537	2.963_3	Not
3435	2.824_8	3465	3541	2.973_3	3526	3396	2.795_5	3435	3387	2.7895	3473	3420	2.812_7	determined
3261	2.726_3	3252	3416	2.809_7	3416			3403	3181	2.6977	3401	3229	2.714_1	
		3127			3404	3330	2.757_1	3330	2867	2.6227	3177	2933	2.635_3	
3067	2.665_3	3039	3217	2.709_4	3230									
					3223	3248	2.721_2	3253						
					3196	3109	2.673_8							
			2974	2.643_8	2929									
					2902									
1635			1621			1682			1651			1629		
			1600			1619			1594			1595		

Table 1 Results of the Raman and infrared spectral analysis of pascoite, hummerite, barnesite, metarossite and metahewettite.

List of Figures

List of Tables

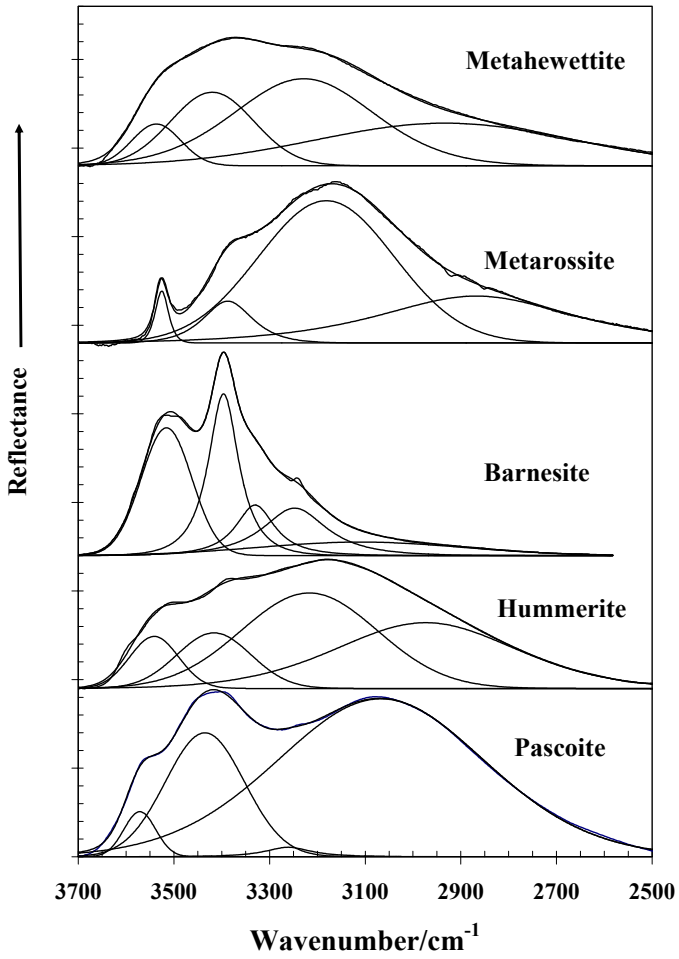
Metahewettite
Metarossite
Barnesite
Hummerite
Pascoite
Reflectance
3700
3500
3300
3100
2900
2700
2500
Wavenumber/cm-1

Figure 1

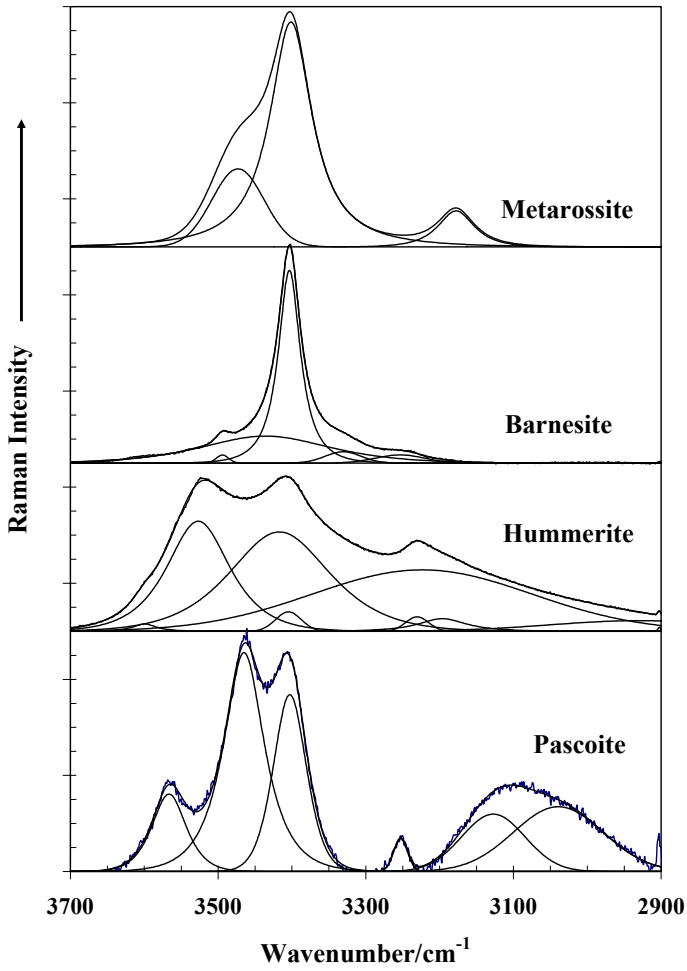
Metarossite
Barnesite
Hummerite
Pascoite
Raman Intensity
3700
3500
3300
3100
2900
Wavenumber/cm-1

Figure 2

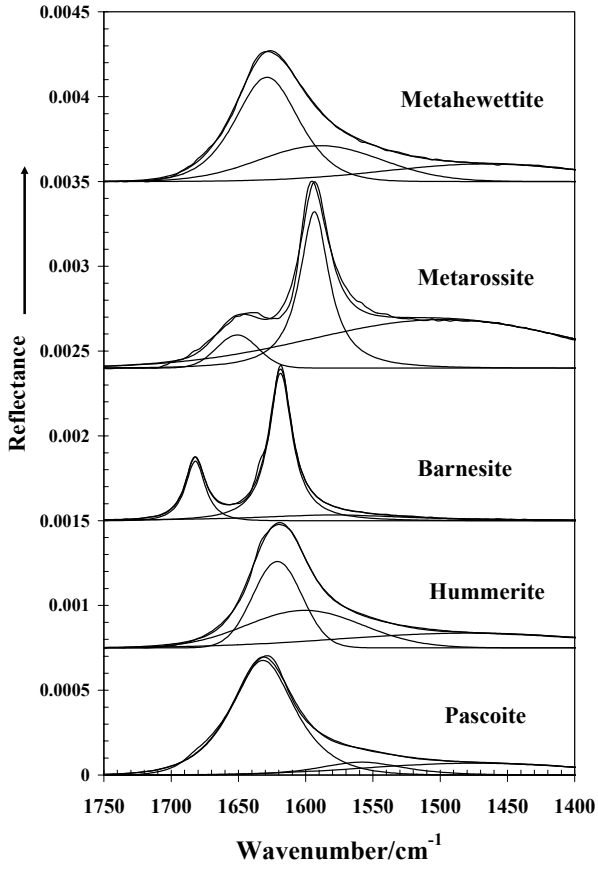
0.0045
0.004
0.0035
0.003
0.0025
0.002
0.0015
0.001
0.0005
0
Reflectance
Metahewettite
Metarossite
Barnesite
Hummerite
Pascoite
1750
1700
1650
1600
1550
1500
1450
1400
Wavenumber/cm-1

Figure 3